Journal of Physical Science and Application 6 (3) (2016) 37-43
doi: 10.17265/2159-5348/2016.03.006

Preparation and Characterization of Electron-Beam Evaporated Cu-InSe Thin Films Using Two Stage Processes

Md. Ariful Islam[1], Md. Nuruzzaman[1], Ratan Chandra Roy[2], Jaker Hossain[2], Md. Julkarnain[2] and K. A. Khan[2]

1. Department of Physics, Rajshahi University of Engineering & Technology, Rajshahi-6204, Bangladesh

2. Department of Applied Physics & Electronic Engineering, University of Rajshahi, Rajshahi-6205, Bangladesh

Abstract: CIS (Cu-InSe) thin films were prepared onto glass substrate by the two stage process—generally called *bilayer* process. At first, Cu layer was deposited onto glass substrate by electron beam evaporation technique and then InSe single layer was deposited on the resulting Cu layer to produce CIS thin film. XRD (X-ray diffraction) analysis revealed that deposited film has an amorphous nature. Electrical resistivity measurements were carried out as a function of temperature during heating and cooling cycles in air. The heating and cooling cycles of the sample are almost reversible after successive heat-treatment in air. In order to consider the influence of the InSe upper layer on the optical properties, the thickness of the InSe upper layer in the CIS films was varied from 50 to 150 nm. Analysis of the transmittance and reflectance spectra, recorded in the wavelength range of 400-1,100 nm, revealed that the CIS films have high absorption coefficient of ~10^4 cm^{-1}. The direct band gap varies from 1.40 to 1.22 eV. The refractive index, the extinction coefficient and the dielectric constant of the CIS films depend on the film thickness.

Key words: CIS, thin film, electron beam, activation energy, absorption coefficient, optical band gap.

1. Introduction

Recently, the ternary semiconductors of the type I-III-VI2 have attracted much attention because of their potential applications in a variety of opto-electronic devices. Among these, CIS (copper indium selenide) can be used as an absorber layer in thin film solar cells because of its high absorption coefficient (~10^4 cm^{-1}), direct band gap (1.04 eV), long term thermal, environmental and electrical stability [1-5]. Its high absorption coefficient and good opto-electrical properties make this compound a major candidate for the next generation solar cells. $CuInSe_2$ based solar cells have already achieved efficiencies of 19.9% for single cell device [6]. Copper indium selenide material crystallises in a chalcopyrite structure [7] which has a diamond like lattice with a face centered tetragonal unit cell. However, the fundamental limitations still exist which prevent large scale industrial applications. The limitation is due to the low band gap value (~1.04 eV) compared to the theoretical optimum value of 1.50 eV. This prevents devices based on these materials from reaching their maximum expected efficiencies [8].

The physical properties of CIS films such as microstructure, electrical and optical properties depend on the deposition methods and experimental conditions. A variety of deposition techniques have been employed by the researchers for the preparation of CIS thin films, such as sputtering [2, 9], electrodeposition [10, 11], spray pyrolysis [12], hot wall deposition [13], thermal co-evaporation [14] etc. Basul et al. used the two-stage process for the deposition of polycrystalline thin films for solar cell applications [15]. This work demonstrated that high quality, single phase $CuInSe_2$ films obtained by selenizing evaporated or electroplated Cu/In stacked layers. Yoon et al. deposited polycrystalline copper

Corresponding author: Md. Ariful Islam, assistant professor, research field: thin film.

indium diselenide thin films on glass or ITO glass substrates by two-stage MOCVD (metal organic chemical vapor deposition) using Cu-and In/Se-containing precursors [16].

In the present study, we have deposited CIS thin films onto glass substrate by e-beam evaporation technique through the two-stage process using two distinctive sources of Cu and InSe. We have discussed the effect of heat treatments on the electrical resistivity of the as-deposited CIS film. Effect of thickness of InSe upper layer on the optical properties was also investigated.

2. Experimental Details

CIS (Cu-InSe) thin films for all the experimental investigations were prepared by e-beam (electron beam) bombardment technique in vacuum at ~ 3×10^{-4} Pa using Edwards E-306 vacuum coating unit. This unit consists of a deposition chamber, a pumping system and electrical sources. The deposition chamber is evacuated with oil diffusion pump. The coating unit is provided with EBS power supply unit having HT (high tension) 0-6 kV and LT (low tension) 0-500 mA. CIS thin films were deposited onto glass substrate from bulk Cu, and InSe granular powder (99.999% pure) obtained from Materials by Metron, USA. A two-stage process was used to prepare CIS thin films. At first stage, Cu thin layer has been prepared onto glass substrate at pressure ~ 3×10^{-4} Pa and then InSe single layer was deposited on the resulting Cu films to produce CIS thin film at that same pressure. When the chamber pressure was reduced ~ 3×10^{-4} pa, deposition was started with different beam currents for different materials by turning on the LT switch.

The film thickness was determined by the Tolansky interference method [17] with an accuracy of ±5 nm. The bottom layer Cu thickness was fixed at 100 nm and the thickness of InSe upper layer was varied from 50 nm to 150 nm. Structural properties of the CIS film were carried out in a PHYLIPS PW3040 X'Pert PRO XRD System. The surface morphology of the films was studied using in a HITACHI S-3400N (SEM) system. The electrical contacts required for resistivity measurements were made with silver paste (leading silver D-200) above the InSe thin films. Van-der-Pauw technique [18] has been used for the measurements of resistivity of thin films. The optical transmittance and reflectance spectra were recorded using a SHIMADZU UV-double beam spectrophotometer at room temperature in the wavelength range of 400-1,100 nm. To determine the band gap of the CIS thin films optically, the plot of $(\alpha h\nu)^2$ vs. $(h\nu)$ was drawn for direct allowed transition. The band gap was determined for the tangent of these curves which intersects the energy axis. Refractive index and dielectric constants of the films were calculated from the transmittance and reflectance measurements.

3. Experimental Results

3.1 Structural and Morphological Characterization of CIS Thin Films

Fig. 1 shows the XRD pattern of the as-deposited CIS thin films of thickness 200 nm, where the thickness of Cu bottom layer is 100 nm. The absence of any remarkable peaks in the XRD pattern indicates that prepared CIS film is an amorphous one.

Fig. 2 displays the SEM (scanning electron microscope) micrographs of the as-deposited CIS thin films of thickness 200 nm. The SEM image shows a uniform surface morphology and grains are distributed throughout the film surface.

3.2 Effect of Temperature on Resistivity and Activation Energy

Temperature dependence of electrical resistivity was measured in the temperature range 300 to 455 K using a standard four-probe setup.

Fig. 3 shows the variation of resistivity as a function temperature during heating-cooling cycles for the as-deposited CIS thin film of thickness 200 nm. It is seen that the heating and cooling cycles are almost

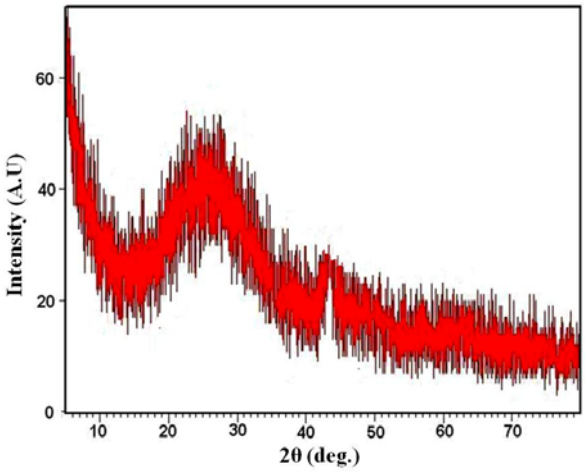

Fig. 1 X-ray diffraction spectra of the as-deposited CIS thin films of thickness 200 nm.

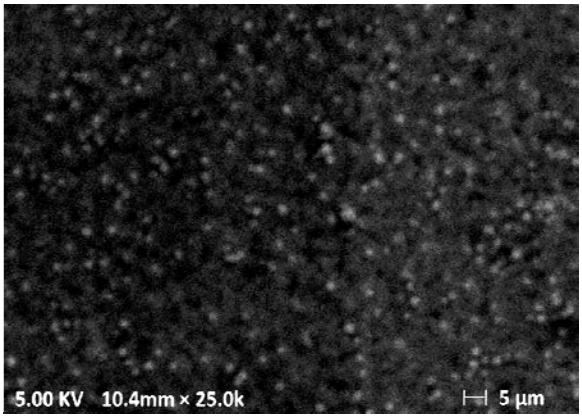

Fig. 2 SEM micrographs of the as-deposited CIS thin film of thickness 200 nm.

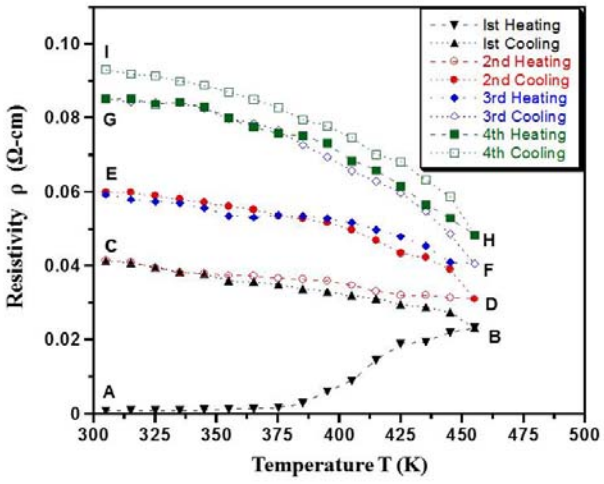

Fig. 3 Variation of electrical resistivity as a function temperature during the heating-cooling cycles.

reversible after four cycles of operation in the investigated temperature range.

During the first heating cycle AB, the resistivity of the as-deposited CIS thin films increases with the increases in temperature. The rise in resistivity with increasing temperature of the film resulted mainly from a decrease in free-carrier concentration and Hall mobility. The decrease in carrier concentration and Hall mobility may be attributed to the electron-electron interactions and ionized impurity scattering. During the first cooling cycle BC, the resistivity increases with the decrease in temperature but does not follow the heating cycle BA, and the film shows an upward tendency of resistivity. During the first heating cycle the film exhibits a metallic behavior with a positive TCR (temperature coefficient of the resistivity), whereas during the first cooling cycle, the film displays a semiconductor-like behavior with negative TCR. In the second step of heat treatment, the heating cycle is shown by CD which shows that the resistivity decreases with the increase in temperature and this reduction in resistivity is associated with thermally activated conduction process which leads to increase in carrier concentration. During the second cooling cycle DE, the variation of resistivity is nearly the same as that during the first cooling cycle.

In third cycle, almost similar behavior is observed like that of second cycle. Finally, in the fourth cycle, it is important to note that the cooling cycle HI, almost follows the heating cycle GH. Therefore the experiment shows that the resistivity of CIS thin films becomes almost reversible after four series of successive heating and cooling cycles.

Dependence of temperature on the conductivity of semiconductor material is expressed by the equation

$$\sigma = \sigma_0 \exp(-\Delta E/2K_B T) \quad (1)$$

where ΔE is the activation energy for the thermally activated process, σ_0 is the pre-exponential factor and K_B is the Boltzmann constant and T is the absolute temperature. Fig. 4 shows the Arrhenius plot of ln (σ) vs. 1000/T of CIS thin film during the fourth heating and cooling cycle.

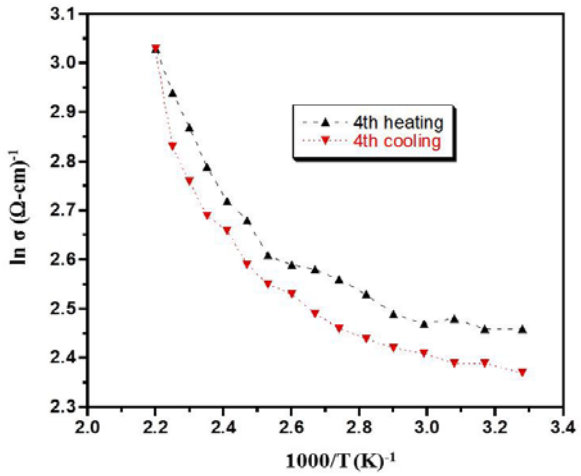

Fig. 4 Arrhenius plot of ln (σ) versus 1000/T of CIS thin film during the fourth heating and cooling cycle.

From the figure, it is seen that the conductivity increases with the increase of temperature indicating the semiconducting behavior.

The conductivity is found to increase with increase in temperature which is associated with a thermally activated process. The activation energies of the films were calculated from the linear-least square fit of the Arrhenius plots. The plot is found to have two regions with two different slops. The activation energies associated with the e-beam evaporated CIS films at two different temperatures are shown in Table 1. Activation energy is found to increase with the increase in temperature. Therefore, it can be assumed that at higher temperature carriers are activated to the localized states. The increase in activation energy with temperature indicates the conduction moves away from the states near the Fermi level.

3.3 Optical Characterization

Optical properties of the films were carried out in the wavelength (λ) range 400 ≤ λ ≤ 1,100 nm using a "UV-Visible SHIMADZU double beam spectrophotometer" at room temperature. Figs. 5a and 5b show the transmittance (% *T*) and absorptance (% A) spectra of the CIS thin films prepared with various thicknesses of 150, 200 and 250 nm, where the thickness of Cu bottom layer is 100 nm. Optical transmittance acquires the maximum at 1,100 nm. Then,

Table 1 Activation energies of CIS thin film during the fourth heating and cooling cycle.

Thickness (nm)		Heat treatment	Activation energies, ΔE (eV)	
			Temperature ranges	
Cu	InSe		300-335 K	400-435 K
			ΔE	ΔE
100	100	4^{th} Heating	0.06	0.22
		4^{th} Cooling	0.03	0.17

the transmittance gradually decreases in the lower wavelength region.

The decrease of transmittance in the higher photon energy region may be due to absorption by free carriers. Transmittance of the films depends on the upper layer InSe films thickness; the transmittance of the thinner film is found to be higher than that for thicker films. From Fig. 5b, it is seen that all the films exhibit high absorption (40%-45%) in the range of 400-600 nm and absorption edge shifts towards the higher wavelength region.

Absorption coefficient (α) of the films is calculated using the relation

$$\alpha = 1/d\ [\ln(1/T)] \quad (2)$$

where *T(λ)* is the transmittance, R(λ) is the reflectance and d is the film thickness. The high absorption coefficient for all films is found to be order of 10^4 cm^{-1} in the 400-600 nm wavelength range. The absorption coefficient data were used to determine energy gap (E_g) using the relation [17]:

$$\alpha h\upsilon = A(h\upsilon - E_g)^{1/2} \quad (3)$$

where hν is the photon energy and A is a constant depending on the transition probability. Optical band gap was obtained for the CIS films from the absorption coefficient versus photon energy by extrapolation of the linear region of the plot to zero absorption (αhυ=0), according to direct allowed transitions.

The plot of $(\alpha h\upsilon)^2$ versus hν for the as-deposited CIS film with different thicknesses is shown in Fig. 6. It is found that direct band gap decreases from 1.40 to 1.22 eV as the thickness of InSe upper layer increases which are closed to the value quoted in Refs. [19, 20]. This decrease in band gap with thickness may be due

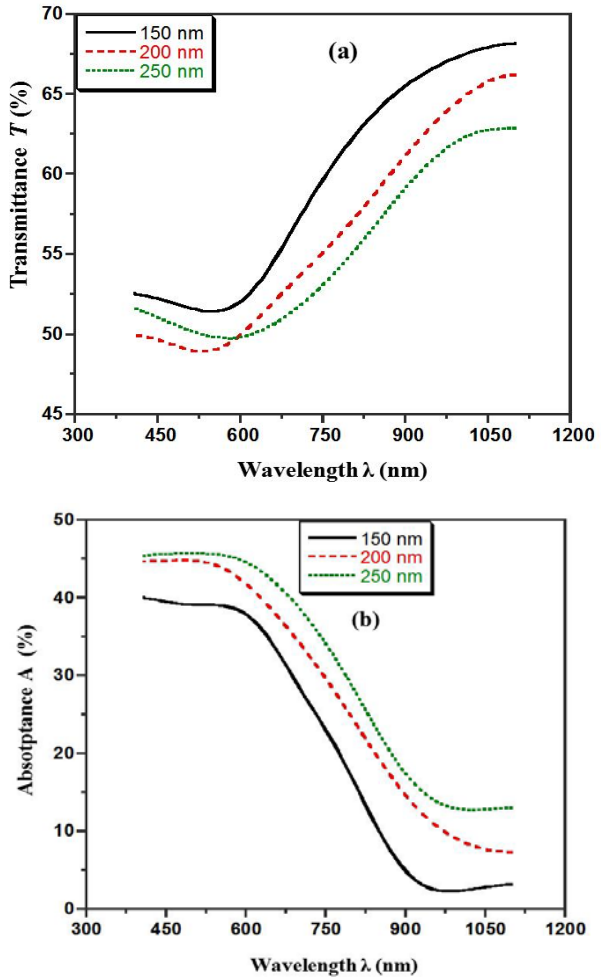

Fig. 5 (a) Optical transmittance and (b) absorptance spectra of the CIS films with different thicknesses of 150 nm, 200 nm and 250 nm, where the thickness of the InSe upper layer varies from 50 to 150 nm.

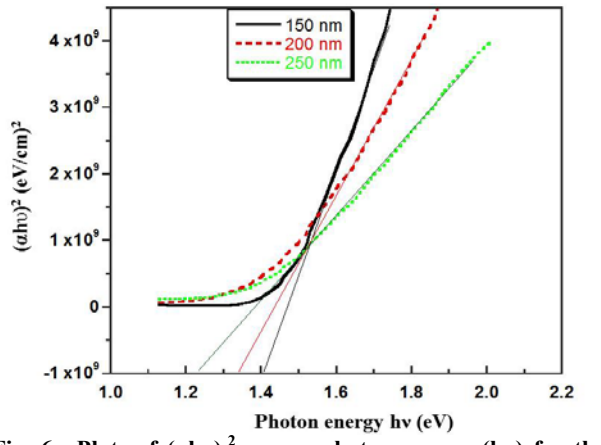

Fig. 6 Plots of $(\alpha h\upsilon)^2$ versus photon energy ($h\upsilon$) for the as-deposited CIS film of thickness 150 nm, 200 nm and 250 nm, where the thickness of the InSe upper layer varies from 50 to 150 nm.

to an increase in grain size and decrease in strain and dislocation density in CIS films.

The reflectivity may be expressed in terms of the real refractive index (n) and extinction coefficient (k) by Ref. [21]

$$R = [(n-1)^2+k^2]/ [(n+1)^2+k^2] \quad (4)$$

The extinction coefficient was calculated using formula, $k = \alpha\lambda/4\pi$. The extinction coefficient is a measure of the fraction of light lost due to scattering and absorption per unit distance of the medium [21].

Figs. 7a and 7b present the variation of refractive index and extinction coefficient of the as-deposited CIS films of different thicknesses with the wavelength of the incident photon. It is observed that refractive

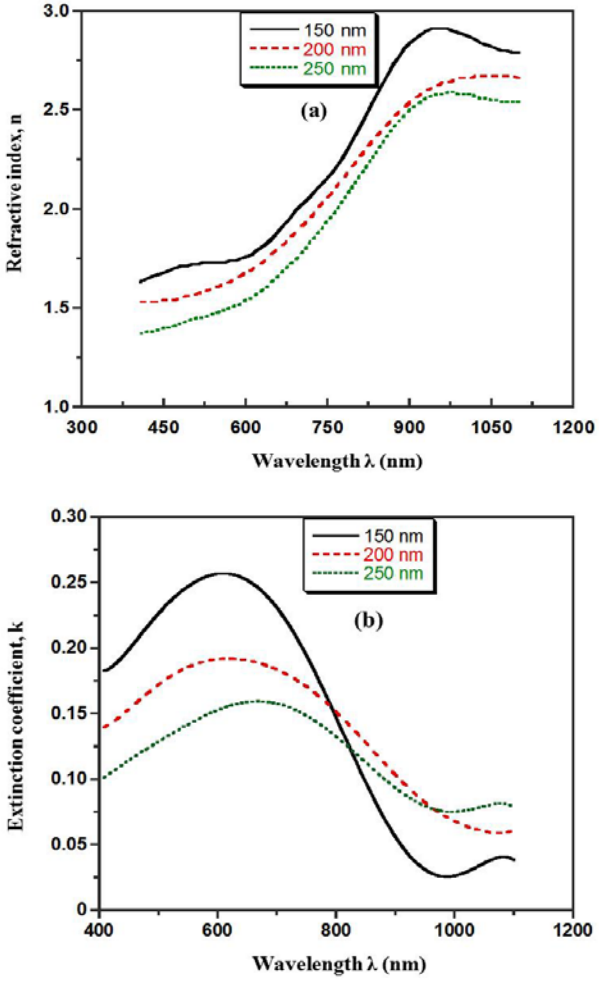

Fig. 7 Variation of (a) refractive index and (b) extinction coefficient as a function of wavelength for the CIS film of different thicknesses.

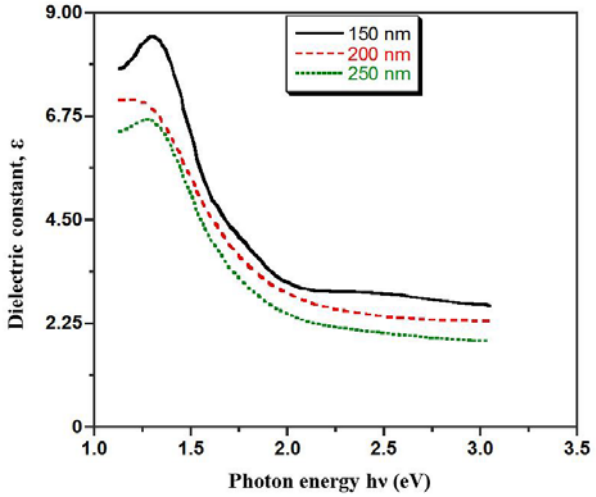

Fig. 8 Dielectric constant vs photon energy for CIS thin films with different thicknesses.

index decreases with film thickness. It varies from 1.70 to 1.40 at the wavelength of 500 nm. The obtained refractive index values are lower than the values obtained by Shah et al. [22]. The refractive index and the extinction coefficient may be correlated with the increase in the absorption coefficient. The decrease in k with the increases in wavelength exhibits that the fraction of light lost due to scattering and consequently decreasing absorption.

The complex dielectric constant ε is given by the relation [23]

$$\varepsilon_r = n^2\text{-}k^2 \quad (5)$$

Fig. 8 shows the photon energy dependence of the complex dielectric constant for CIS thin films with different films thicknesses. It is obvious that the dielectric constant decreases with increase in film thickness.

4. Conclusions

CIS thin films were prepared onto glass substrate by e-beam evaporation technique. XRD pattern indicated that deposited CIS film is amorphous in nature. The effect of temperature on the electrical resistivity of CIS thin films was studied in the 300-455 K temperature range during heating and cooling cycles. Metallic behavior turns into semiconductor after heating the sample and the heating and cooling cycles are almost reversible after successive of heating-cooling operations in air. Effect of the thickness of InSe upper layer on the optical properties of CIS films was investigated in the wavelength range of 400-1,100 nm. Analysis of the transmittance and the reflectance spectra of CIS films revealed that all films have high absorption coefficient of ~10^4 cm^{-1} in the 400-600 nm wavelength range. The direct optical band gap is found to vary between 1.40 eV and 1.22 eV for various thickness. The refractive index and the dielectric constant of these films depend on the film thickness. Both the high optical absorption coefficient and the high band gap make the CIS films a promising candidate for high efficiency absorber layer in thin film solar cells and other possible optoelectronic applications.

Acknowledgments

The authors are thankful to the Head, Department of applied Physics & Electronic Engineering, University of Rajshahi, Bangladesh, for providing laboratory facilities. The authors also are thankful to the Institute of Mining, Mineralogy & Metallurgy, BCSIR, Joypurhat, Bangladesh for measuring X-ray data.

References

[1] Postnikov, A. V., and Yakushev, M. V. 2004. "Lattice Dynamics and Stability of $CuInSe_2$." *Thin Solid Films* 451 (3): 141-4.

[2] Muller. J., Nowoczin. J., and Schmitt, H. 2006. "Composition, Structure and Optical Properties of Sputtered Thin Films of $CuInSe_2$." *Thin Solid Films* 496 (2): 364-70.

[3] Schon, J. H., Alberts, V., and Bucher, E. 1997. "Structural and Optical Characterization of Polycrystalline $CuInSe_2$." *Thin Solid Films* 301 (6): 115-21.

[4] Shah, N. M., Ray, J. R., Kheraj, V. A., Desai, M. S., Panchal, C. J., and Rehani, B. 2009. "Structural, Optical, and Electrical Properties of Flash-Evaporated Copper Indium Diselenide Thin Films." *J. Material Science* 44 (January): 316.

[5] Babo, S. M., Dhanasekaran, R., and Ramasamy P. 1991. "Thin Film Deposition and Characterization of $CuInSe_2$."

Thin Solid films 198 (5): 269-78.

[6] Repins, I., Contreras, M. A., Egaas, B., DeHart, C., Scharf, J., Perkins, C. L., To, B., and Noufi, R. 2008. "19.9%-Efficient ZnO/CdS/$CuInGaSe_2$ Solar Cell with 81.2% Fill Factor." *Progress in Photovoltaics Research and Applications* 16 (3): 235.

[7] Shay, J. L., and Wernick, J. H. 1975. *Ternary Chalcopyrite Semiconductors: Growth, Electronic Properties and Applications.* New York: Pergamon.

[8] Ahmed, E., Tomlinson, R. D., Pilkington, R. D., Hill, A. E, and Ahmed, W. 1998. "Significance of Substrate Temperature on the Properties of Flash Evaporated $CuIn_{0.75}Ga_{0.25}Se_2$ Thin Films." *Thin solid films* 335 (11): 54-8.

[9] Guang-Xing, L., Zhuang-Hao, Z., Xing-Min, C., and Dong-Ping, Z. 2010. "Adjustment of the Selenium Amount during Ion Beam Sputtering Deposition of CIS Thin Films." *J. Materials Science: Materials in Electronics* 21 (9): 897-901.

[10] Feng, K., Ao, J. P., Sun, G. Z., He, Q., and Sun, Y. 2009. "Structure and Photovoltaic Characteristics of $CuInSe_2$ Thin Films Prepared by Pulse-Reverse Electrodeposition and Selenization Process." *J. Alloy and Compound* 478 (1-2): L25-27.

[11] Hung, P. K., Huang, C. H., and Houng, M. P. 2014. "Enhancing the Performance of Electrodeposited $CuInSe_2$ Solar Cells by Suppressing Secondary Phases Using Sodium Dodecyl Sulphate." *J. Materials Science: Materials in Electronics* 25 (4):1848-55.

[12] Alaa, A. A., and Afify, H. H. 2008. "Growth, Microstructure, Optical and Electrical Properties of Sprayed $CuInSe_2$ Polycrystalline Films." *Materials Research Bulletin* 43 (6): 1539-48.

[13] Agilan, S., Mangalaraj, D., Narayandass, N. S., Rao, G. M., and Velumani, S. 2010. "Structure and Temperature Dependence of Conduction Mechanisms in Hot Wall Deposited $CuInSe_2$ Thin Films and Effect of Back Contact Layer in $CuInSe_2$ Based Solar Cells." *Vacuum* 84 (10): 1220-25.

[14] Bhuiyan, M. A. S., Bhuiyan, A. S., Hossain, A., and Mahmood, Z. H. 2013. "Studies on Optical Characteristics of $CuInSe_2$ Thin Films." *Central European Journal of Engineering* 3 (2): 170-3.

[15] Basol, B. M., and Kapor, V. K. 1990. "Deposition of $CuInSe_2$ Films by a Two-Stage Process Utilizing E-Beam Evaporation." *IEEE Transactions on Electron Devices* 37 (2): 418-21.

[16] S. H. Yoon, Seo, K.W., Lee, S. S., and Shim, Il. W. 2006. "Preparation of $CuInSe_2$ Thin Films through Metal Organic Chemical Vapor Deposition Method by Using Di-μ-Methylselenobis (Dimethylindium) and Bis(ethylisobutyrylacetato) Copper (II) Precursors." *Thin Solid Films* 515 (4): 1544-7.

[17] Tolansky, S. 1948. *Multiple-beam Interference of Surfaces and films*. London: Clarendon Press.

[18] Van der Pauw, L. J. 1958. "A Method of Measuring Specific Resistivity and Hall Effect of Discs of Arbitrary Shape." *Philips Research Reports* 13: 1-9.

[19] Castaneda, S. I., and Rueda, F. 2000. "Differences in Copper Indium Selenide Films Obtained by Electron Beam and Flash Evaporation." *Thin Solid Films* 361-362 (2): 145-9.

[20] Lia, L., Maa, Y., Gaoa, G., Wanga, W., Guob, S., Youa, J., and Xie, J. 2016. "Fabrication and Characterization of Copper-Indium-Diselenide ($CuInSe_2$, CIS) Thin Film Using One-Step Electro-Deposition Process." *J. Alloys Compound* 658 (February): 774-9.

[21] Heavens, O. S. 1965. *Optical Properties of Thin Solid Films*. New York: Dover Publications.

[22] Shah, N. M., Panchal, C. J., Kheraj, V. A., Ray, J. R., and Desai, M. S. 2009. "Growth, Structural and Optical Properties of Copper Indium Diselenide Thin Films Deposited by Thermal Evaporation Method." *Solar Energy* 83 (5): 753-60.

[23] Ali, M. O. 1993. *Elementary Solid State Physics*. Boston: Addison-Wesley Publishing Company.